 CMC, vol.51, no.3, pp.203-215, 2016

A Numerical Study Comparing The Effect on Residual Stresses of Two Different Types of Projectiles During Shot Peening

J. Solórzano-López[1], F.A. García-Pastor[2], Angélica Flores-Luna[3]

Abstract: Shot peening is a widely used technique to improve fatigue life in metallic alloys. This processing technique introduces a subsurface compressive residual stress field through a plastic deformation of the surface caused by the impact of a large number of high-speed projectiles. There are a number of parameters that affect the residual stress field depth and magnitude. The effects of the impact angle, shot speed and shot geometry are currently being researched. In particular, substituting spherical cast shots by cylindrical cut wire shots is an attractive option, especially in terms of cost. The effect of shot geometry on residual stresses, however, needs to be further investigated. Because industrial-scale experimentation is costly and cumbersome, mathematical modeling offers a convenient alternative to carry out this type of research.

The present work shows a comparison between the residual stresses generated by the impact of spherical and cylindrical projectiles on a steel substrate. This three-dimensional model was developed using ABAQUS finite element commercial software (Release 6.12, Dassault Systémes, France). The results show that cylindrical shots generate residual stress fields that are higher in magnitude than those generated by a spherical shot. However, the residual stress field of cylindrical shots impacting the surface at an oblique angle shows an important degree of asymmetry. This effect is not found when spherical shots impact the surface at the same oblique angle.

Keywords: Shot Peening, Finite element method, Residual Stresses.

[1] UNAM, Facultad de Química, Ciudad de México, México
[2] Cinvestav Unidad Saltillo, Coahuila, México
[3] TecNM, Instituto Tecnológico de Tláhuac III, Ciudad de México, México

1 Nomenclature

$\mathbf{a}$	Acceleration
$\mathbf{A_1, A_2, B, C, n, m,}\sigma_\mathbf{O}$	Material parameters
$\mathbf{C_O}$	Speed of sound in the material
$\mathbf{C_V}$	Specific heat at constant volume
$\mathbf{E}$	Internal energy
$\mathbf{R_C}$	Rockwell C hardness of material
$\mathbf{S}_\alpha$	Linear Hugoniot slope coefficient
$\mathbf{s, v}$	Terms of motion equation
$\mathbf{t}$	Time
$\mathbf{T}$	Temperature
$\mathbf{T_r}$	Reference temperature
$\mathbf{T_m}$	Melting temperature
$\mathbf{T^*}$	Dimensionless temperature
$\mathbf{V_O}$	Reference specific volume
$\mathbf{\Gamma_O}$	Gruneisen's gamma at reference state
$\dot{\boldsymbol{\varepsilon}}_\mathbf{O}$	Reference strain rate
$\boldsymbol{\varepsilon}_\mathbf{P}$	Equivalent plastic strain
$\dot{\boldsymbol{\varepsilon}}$	Plastic strain rate
$\dot{\boldsymbol{\varepsilon}}^*$	Dimensionless strain rate
$\boldsymbol{\eta}$	Dimensionless density
$\boldsymbol{\rho}$	Density
$\boldsymbol{\rho}_\mathbf{O}$	Initial density
$\boldsymbol{\sigma}_\mathbf{y}$	Johnson-Cook model term
$\boldsymbol{\omega}_\mathbf{max}$	Maximum eigenvalue of the system

2 Introduction

Shot peening is a widely used technique to improve fatigue properties in metallic alloys. In this process, a large amount of projectiles impacts the component surface at high velocity. This impact produces a surface plastic deformation, which in turn generates a compressive residual stress field [Guagliano (2001); Wang, Platts, and Levers (2002)]. These compressive residual stresses increase the component fatigue life because a compressive stress field hinders the propagation of surface and sub-surface cracks [Guagliano (2001); Shivpuri, Cheng, and Mao (2009)]. This effect is a function of both the depth and magnitude of the residual stress field, as well as the final surface quality. It is only through the adequate balance of these factors that fatigue life can be maximized.

Conducting a parametric analysis of the shot peening process in an industrial scale can be extremely expensive in terms of consumables, specialized technicians and non-productive time. Additionally, to analyze the effect of processing parameters in the residual stress field, it is mandatory to use specialized equipment to measure residual stresses, such as X-ray diffractometers [Shivpuri, Cheng, and Mao (2009); Majzoobi, Azizi, and Alavi Nia (2005); Meguid, Shagal, and Stranart (2007)]. Because of these reasons, numerical simulation using finite element modeling offers a cost-effective alternative.

Finite element modeling (FEM) is a very powerful tool to numerically solve the equations governing mechanical deformation [Murthy, Iyer, and Raghu-Prasad (2012); Panthi and Saxena (2012)]. While several analytical solutions have been proposed to analyze residual stress fields after shot peening [Shen and Atluri (2006); Bhuvaraghan, Srinivasan, Maffeo, and Prakash (2010)], FEM appears to be a very appealing alternative to study this particular process.

In general, a shot peening model should include the governing equations for the target and shot as well as the general movement equation. Several finite element models have been proposed, including various parametric analyses and solution algorithms. Some authors have developed computational models built from scratch with a very detailed approach regarding the governing equations [Barrios, Ángelo, and Gonçalves (2005)]. However, most of the published models are developed on commercial software such as ABAQUS, both with the built-in solver and with tailor-made add-ons such as heat transfer subroutines [Levers and Prior (1998)]. ABAQUS has an explicit approach to solve the governing equations explicitly, and it is widely regarded as the most adequate algorithm to carry out dynamic phenomena calculations [Guagliano (2001); Mylonas and Labeas (2011); Shivpuri, Cheng and Mao (2009); Meguid, Shagal, and Stranart (2007); Levers and Prior (1998); Kim, Lee, Lee, and Cheong (2010)]. The model published by Zimmermann [Zimmermann, Schulze, Baron and Löhe (2008)] thoroughly describes the governing equations that describe the mechanical behavior of the target. It also reports the development of a user subroutine that was added to ABAQUS to improve its solution capabilities. The model presented by Rouhaud [Rouhaud, Ouakka, Ould, Chaboche, and Francois (2005)] shows a parametric study in which the processing conditions are changed over a relatively large range. However, this model is limited to two dimensions. Finally, Werke [Werke (2008)] presented a detailed literature review of mathematical models aimed at finding optimal processing conditions. This review is summarized in two tables: one describes the target conditions, and the other displays the shot parameters. The conclusions presented offer a practical analysis of processing parameters such as impact velocity, shot diameter and friction factors.

The cited works show that several research efforts have been made to characterize optimal shot peening processing parameters through mathematical modeling. However, most papers found in the specialized literature only show simulations of spherical projectiles, while the use of cylindrical cut wire shots is a very common industrial practice. This is mainly because cut wire shots are significantly cheaper than cast shots. Current numerical simulations are limited in the number of impacts. Although it has been shown that it is possible to simulate a flow of hundreds of shots, this can only be done in the flow itself to analyze peening coverage because a fully coupled CFD + FEM simulation would be prohibitive in terms of numerical convergence [Nguyen, Poh, and Zhang (2014)]. Because of these limitations, in this paper, only 4 shots were simulated using spheres, cylinders and a combination of both. While this number of impacts is far smaller than current industrial practice, a reasonably good approximation in terms of residual stress field characteristics can be obtained.

This work shows the results of shot peening simulations comparing cylindrical and spherical shots as well as the impact angle (45° and 75°). The effect of the shot geometry on the residual stress field was assessed in both depth and magnitude of the compressive stress field. Final surface quality was not assessed in this particular paper because a proper simulation with the hundreds of impacts that would be required to analyze the surface condition was excessively demanding in terms of computing time. The simulation results were analyzed to assess the residual stress field depth, shape and magnitude.

3 Mathematical Model

The proposed mathematical model makes a parametric analysis of the shot geometry and impact angle. Figure 1 shows the geometrical arrangement of the mathematical model for cylindrical and spherical shots. In both cases, 4 simultaneous shots were simulated. Four different parametric conditions were simulated. These conditions are presented in table 1.

3.1 Assumptions

a) The target material is considered to be a deformable body with elasto-plastic characteristics.

b) The shots are non-deformable rigid bodies; therefore, their mechanical response after the impact was not simulated.

c) Simulations are carried out for a long enough time to allow for stabilization of the target material, when the internal stresses are no longer changing.

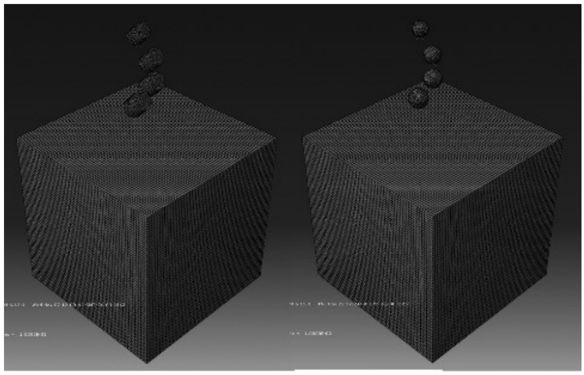

Figure 1: Geometrical arrangement of the mathematical model with a) cylindrical and b) spherical shots.

Table 1: Parametric conditions simulated in the model

Simulation	**Munition**	**Impact angle [°]**
1	Spheres	45
2	Cylinders	45
3	Spheres and Cylinders	75

3.2 Governing equations

The governing equations of the shot peening numerical model are presented in Table 2. These equations were solved using integration of the central differences explicit method. In all of the equations presented, v represents velocity, a represents body acceleration, and t represents time. The incremental steps are indicated by the subindex.

Because the algorithm solution is explicit, the time step is limited by equation 2 in table 2. The limiting term ω is the maximum Eigenvalue of the system. Equation 3 describes the Johnson-Cook empirical model and its parameters. This model describes the high impact tensile rates and is specific for a particular material. To take into account the wave propagation effect in the hydrodynamic pressure during the impact, the Mie-Gruniesen equation was included (equation 4 in table 2). This equation is a function of the internal energy, which is calculated through equation 5 [Hong, Ooi, and Shaw (2008); Bhuvaraghan, Srinivasan, Maffeo, McLain, Potdar, and Prakash (2010); Shivpuri, Cheng, and Mao (2009); Miao, Larose, Perron, and Lévesque (2009)].

Table 2: Governing equations

$v^{(i+1/2)} = v^{(i-1/2)} + \frac{\Delta t^{(i+1)} + \Delta t^{(i)}}{2} a^{(i)}$ $s^{(i+1)} = s^{(i)} + \Delta t^{(i+1)} v^{(i+1/2)}$	1. Motion equations
$\Delta t \leq \frac{2}{\omega_{\max}}$	2. Time increment
$\sigma_y = (\varepsilon_p, \dot{\varepsilon}, T) = \sigma_0 \left[1 + \frac{B}{\sigma_0}(\varepsilon_p)^n\right]$ $\left[1 + C\ln(\dot{\varepsilon^*})\right]\left[1 - (T^*)^m\right]$ $\dot{\varepsilon^*} = \frac{\dot{\varepsilon}}{\dot{\varepsilon}_0}$ $T^* = \frac{(T - T_r)}{(T_m - T)_r}$ $\sigma_0 = \exp(A_1 R_C + A_2)$	3. Johnson-Cook Model and its parameters
$p = \frac{\rho_0 C_0^2(\eta - 1)\left[\eta - \frac{\Gamma_0}{2}(\eta - 1)\right]}{\left[\eta - S_a(\eta - 1)\right]^2} + \Gamma_0 E$ $\eta = \frac{\rho}{\rho_0}$	4. Hydrodynamic pressure developed during the impact
$E = \frac{1}{V_0}\int C_V dT \approx \frac{C_V(T - T_0)}{V_0}$	5. Internal energy as temperature function

3.3 Boundary conditions

The proposed model boundary conditions are depicted in figure 2. The target is defined as a cube with symmetry conditions on all the faces not being impacted by the shot. The projectiles are moving at a speed of 80 m/s and a variable impact angle of either 45° or 75° These angles were chosen to assess the effect of the angle of impact commonly used in industrial practice (45°) and one closer to perpendicularity (75°).

3.4 Model description

The model was developed using ABAQUS 6.12-1 commercial software with an explicit and dynamical solver. The target was defined as a 1 cm^3 cube defined by a

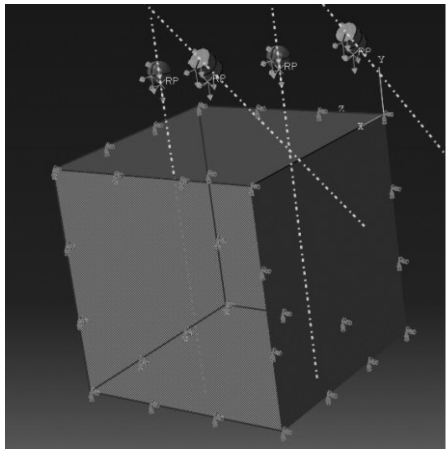

Figure 2: Boundary conditions of the numerical model.

mesh of 296,000 elements. A mesh of approximately 1,300 node elements defined the projectiles. The cylinders were 1 mm in diameter and 1 mm long, and the spheres had a 1 mm diameter.

The target material was defined as low-carbon steel with mechanical properties corresponding to a room temperature of 25°C. Young's modulus was defined as 200×10^9 Pa, while the density was 7858 Kg/m^3. The 6 different simulations shown in table 1 were calculated during 0.01 s of simulated time. The speed of 4 shots was kept constant at 80 m/s.

4 Results and discussion

Figure 3 shows the indentation and residual stresses produced by the impact of cylindrical projectiles at 45°. It can clearly be observed that the indentation does not have a uniform profile, with the target material being pushed to the opposite side of the impact. The residual stresses range from 1.07×10^9 to 6.75×10^7 Pa.

In comparison, figure 4 shows the indentation caused by the impact of spherical projectiles. It is readily apparent that the indentations are more uniform than the ones caused by the impact of cylindrical projectiles. Furthermore, the residual stresses are considerably lower than those from the previous condition, ranging from 6.82×10^8 to 3.81×10^7 Pa.

Figure 5 depicts the results of simulating condition number 6 from table 1 in which two types of projectiles were used. The difference in the residual stress fields caused by cylindrical and spherical shot impacts can be easily observed. Counting from the top, the first and third indentations are caused by cylindrical shots, while the second and fourth ones are the results of spherical shots.

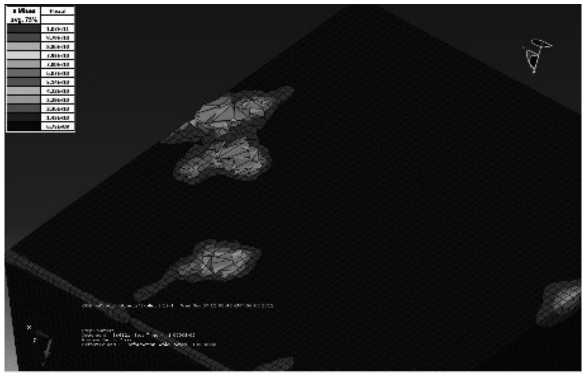

Figure 3: Residual stress fields caused by the impact of cylindrical shots with an impact angle of 45°.

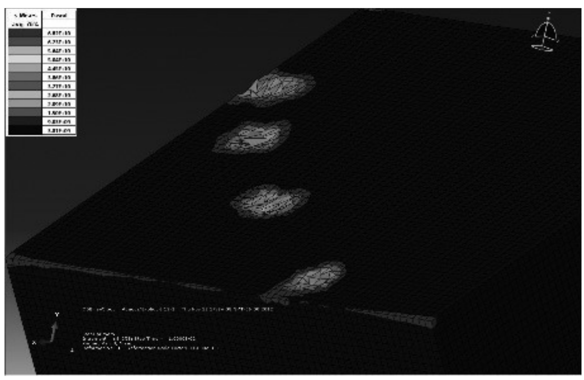

Figure 4: Residual stress fields caused by the impact of spherical projectiles with an impact angle of 45°.

To further investigate the differences between spherical and cylindrical shots, the indentation cross-sections are depicted in figure 6. It is immediately apparent that there is an important difference in the indentation shape and size. The cylindrical shot causes an asymmetrical indentation (figure 6a), while the spherical shot creates a symmetrical crater. It is important to highlight that both indentations were created by projectiles that had an impact angle of 75°. This difference in shape can be explained by the cylindrical shot edge that effectively pushes the material to the impact direction. This effect is shown in figure 7.

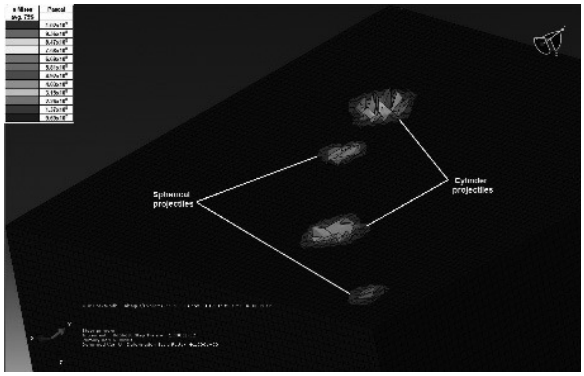

Figure 5: Residual stress fields caused by the impact of both cylindrical (first and third indentations counting from the top) and spherical projectiles (second and fourth).

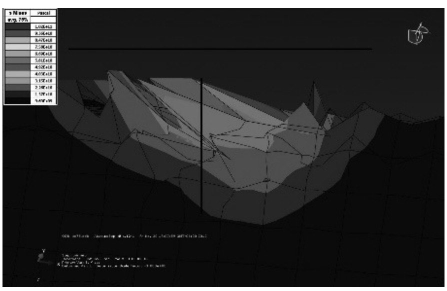

(a)

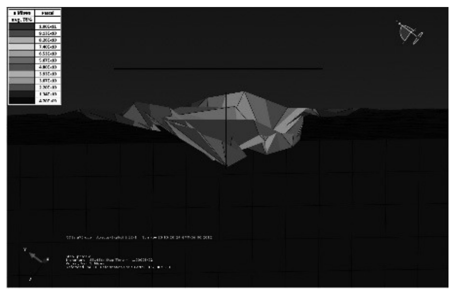

(b)

Figure 6: (a) Indentation cross-sections for impacts at 75° for a) a cylindrical shot. (b) Indentation cross-sections for impacts at 75° for b) a spherical shot.

Residual stress profiles were extracted from the finite element modeling results, plotted against position, and measured along the line that grazes the cavity bottom. To properly compare between the two types of projectiles, the distance was normalized. A comparison of horizontal residual stress profiles between cylindrical and spherical projectiles impacting at 75° is shown in Figure 8(a). It is immediately apparent that there is an important difference in terms of magnitude. Furthermore, despite the impact angle, the residual stress profiles caused by the spherical projectile are clearly symmetrical. This effect is clearly the result of the shot geometry because the masses are almost the same for either projectile type (4.2 mm^3 for the sphere and 3.14 mm^3 for the cylinder). The residual stress field is not only different in shape; the stress magnitude is also significantly higher in the cylindrical

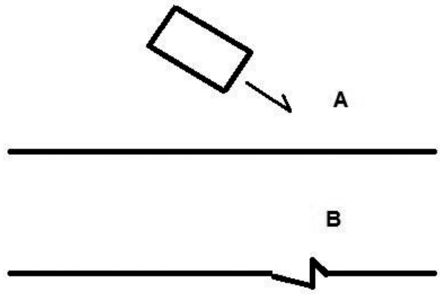

Figure 7: Effect of the cylindrical shot edges in the final indentation shape.

case. This is also the case when comparing vertical stress profiles (shown in Figure 8(b). Additionally, it can be observed that in the case with the spherical projectile, there is a zone in which the residual stress does not immediately increase. In contrast, the vertical stress profile for the impact with a cylindrical projectile decreases monotonically away from the surface.

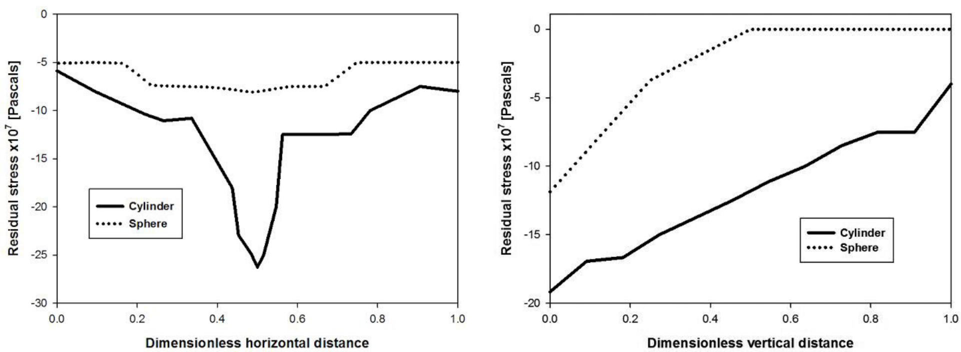

(a) (b)

Figure 8: Residual stress profiles calculated for both spherical and cylindrical projectiles along a central (a) horizontal line and (b) vertical line.

These findings are particularly relevant when compared to the common industrial practice of using angular shots to improve the surface finish. The spherical case is expected to improve the surface finish with no detrimental effects to the residual stress field. The use of cylindrical shots, however, may have an undesirable effect of generating asymmetrical residual stress fields. The effect would need to be experimentally quantified, but the results shown in the present paper suggest that this asymmetry is not negligible. Multiple impacts by cylindrical shots may exacerbate this effect. However, additional simulations and experiments are needed to clarify this issue.

Finally, it is important to highlight the exploratory nature of these results. To obtain a more thorough understanding of the effect of cylindrical shots in the residual stress fields during shot peening, it is necessary to assess the effect of shot conditioning. After several uses, the edges of cylindrical shots are not as sharp as they were originally; this is commonly referred to as shot conditioning. However, such analyses require two computational domains, one for the target and one for the shot in a two-body FE model. These complex models may help to elucidate this effect.

5 Conclusions

- A multi-impact model was developed for shot peening simulations of both cylindrical and spherical projectiles. The results show that there is an important difference in the impacts caused by these two types of projectiles.
- The residual stress field generated by a 75° impact of a cylindrical shot shows an asymmetric horizontal profile.
- In contrast, there are no signs of asymmetry in the residual stress field caused by spherical shots.
- The stress magnitude is significantly higher in the cylindrical shot than the one from the spherical shot.
- The asymmetry in residual stresses caused by the cylindrical shot may have some effects in mechanical properties; however, the extent of these effects needs to be addressed by further investigations.

Acknowledgement: The authors acknowledge the funding from CONACyT through Dr. J. Solórzano-López Postdoc.

References

Barrios, D. B.; Ángelo, E.; Gonçalves, E. (2005): Finite element shot peening simulation for residual stress. Analysis and comparison with experimental results. in: *VIII Congreso Argentino de Mecánica Computacional MECOM 2005*, A. Larreteguy (Editor), Buenos Aires, Argentina, pp. 413–422.

Bhuvaraghan, B. S.; Srinivasan, M.; Maffeo, B.; McLain, R. D.; Potdar, Y.; Prakash, O. (2010): Shot peening simulation using discrete and finite element methods. *Adv. Eng. Softw.*, vol. 41, pp. 1266–1276.

Bhuvaraghan, B.; Srinivasan, S.M.; Maffeo, B.; Prakash, O. (2010): Analytical solution for single and multiple impacts with strain-rate effects for shot peening. *CMES - Computer Modeling in Engineering and Sciences*, vol. 57, no. 2, pp. 137–158.

Guagliano, M. (2001): Relating Almen intensity to residual stresses induced by shot peening: a numerical approach. *J. Mater. Process. Tech.*, vol. 110, pp. 277–286.

Hong, T.; Ooi, J. Y.; Shaw, B. (2008): A numerical simulation to relate the shot peening parameters to the induced residual stresses. *Eng. Fail. Anal.*, vol. 15, pp. 1097–1110.

Kim, T.; Lee, J. H.; Lee, H.; Cheong, S. (2010): An area-average approach to peening residual stress under multi-impacts using a three-dimensional symmetry-cell finite element model with plastic shots, *Mater. Design*, vol. 31, pp. 50–59.

Levers, A.; Prior, A. (1998): Finite element analysis of shot peening. *J. Mater. Process. Tech.*, vol. 80–81, pp. 304–308.

Majzoobi, G. H.; Azizi, R.; Alavi Nia, A. (2005): A three-dimensional simulation of shot peening process using multiple shot impacts. *J. Mater. Process. Tech.*, vol. 164–165, pp. 1226–1234.

Meguid, S. A.; Shagal, G.; Stranart, J. C. (2007): Development and validation of novel FE models for 3D analysis of peening of strain-rate sensitive materials. *J. Eng. Mater-T ASME*, vol. 129, pp. 271–283.

Miao, H. Y.; Larose, S.; Perron, C.; Lévesque, M. (2009): On the potential applications of a 3D random finite element model for the simulation of shot peening. *Adv. Eng. Softw.*, vol. 40, pp. 1023–1038.

Murthy, A.R.; Iyer, N. R.; Raghu-Prasad, B.K. (2012): Fracture analysis of high strength and ultra-high strength concrete beams by using finite element method. *CMC: Computers, Materials & Continua*, vol. 30, no. 2, pp. 177–194.

Mylonas, G. I.; Labeas, G. (2011): Numerical modelling of shot peening process and corresponding products: Residual stress, surface roughness and cold work prediction. *Surf. Coat. Tech.*, vol. 205, pp. 4480–4494.

Nguyen, B. V.; Poh, H. J.; Zhang, Y. W. (2014): Predicting shot peening coverage using multiphase computational fluid dynamics simulations. *Powder Tech.*, vol. 256, pp. 100–112.

Panthi, S. K.; Saxena, S. (2012): Prediction of crack location in deep drawing processes using finite element simulation. *CMC: Computers, Materials & Continua*, vol. 32, no. 1, pp. 15–28.

Rouhaud, E.; Ouakka, A.; Ould, C.; Chaboche, J.; Francois, M. (2005): Finite elements model of shot peening, effect of constitutive laws of the material. in: *Proceedings of the 9th International Conference on Shot Peening 2005*, Paris, France, pp. 107–112.

Shen, S.; Atluri, S.N. (2006) An analytical model for shot-peening induced residual stresses. *Computers, Materials and Continua*, vol 4, no. 2, pp. 75–85.

Shivpuri, R.; Cheng, X.; Mao, Y. (2009): Elasto-Plastic pseudo-dynamic numerical model for the design of shot peening process parameters. *Mater. Design*, vol. 30, pp. 3112–3120.

Wang, T.; Platts, M. J.; Levers, A. (2002): Finite element impact modeling for shot peen forming. in: *Proceedings of the 8th International Conference on Shot Peening 2002*, Garmisch-Partenkirchen, Germany.

Werke, M. (2008): Methods and models for shot peening simulation. in: *Proceedings of the Swedish Production symposium 2008*, Swerea IVF, Molndal, Sweden.

Zimmermann, M.; Schulze, V.; Baron, H. U.; Löhe, D. (2008): A novel 3D finite element simulation model for the prediction of the residual stress state after shot peening. in: *Proceedings of the 10th International Conference on Shot Peening*, Tokyo, Japan, pp. 63–68.